

Research Article

Newly Constructed Subway on Over-Track Bridge Safety and Vibration Reduction Measure

Yuan Xu,¹ Hui Li,¹ Jue Hou,¹ Liming Zhu,² and Lingkun Chen ^{3,4,5}

¹Nanjing Metro Construction Co., Ltd., Nanjing 210098, Jiangsu, China

²College of Transportation Science and Engineering, Nanjing Tech University, Nanjing 211800, Jiangsu, China

³College of Architecture Science and Engineering, Yangzhou University, Yangzhou 225127, Jiangsu, China

⁴Department of Civil and Environmental Engineering, University of California, Los Angeles, 90095, CA, USA

⁵School of Civil Engineering, Southwest Jiaotong University, Chengdu 610031, Sichuan, China

Correspondence should be addressed to Lingkun Chen; lingkunchen08@hotmail.com

Received 12 March 2024; Revised 12 April 2024; Accepted 29 April 2024; Published 16 May 2024

Academic Editor: Chao Zou

Copyright © 2024 Yuan Xu et al. This is an open access article distributed under the Creative Commons Attribution License, which permits unrestricted use, distribution, and reproduction in any medium, provided the original work is properly cited.

Primarily generated at the interface between the wheel and the rail, railroad vibrations then propagate through the supporting soil. If these vibrations reach nearby bridges and buildings, they amplify the vibration nuisance and cause ground noise, which has detrimental effects on nearby residents, sensitive equipment, and historic structures. By analyzing measured data from metro vibration field vibration experiments, this article attempts to contribute to the body of knowledge on environmental vibration propagation patterns by offering insightful conclusions. Before analyzing the deformation response of the metro jet system (MJS) vibration isolation piles to the structure and the ground, we investigated the effect of MJS vibration isolation piles in the ground of the existing subway tunnel structure on the control of vibration of the proximate structure and conducted dynamic tests on the vibration of bridges without vibration isolation measures caused by operating subway trains. The tests determined that the acceleration of the bridge's lateral vibration exceeded the code limit; one of the contributing factors was that the bridge's structure had already sustained damage. The utilization of MJS isolation piles was also discovered to safeguard the extant bridge pile foundations. The paper presents an innovation in the form of economically viable vibration mitigation strategies that were implemented subsequent to the identification that the lateral vibration acceleration of the preexisting bridge surpassed the prescribed code standards. Considerable insight is gained regarding the design and implementation of vibration control systems for structures situated near caverns, encompassing deep foundation works.

1. Introduction

Vibration issues resulting from train operations have garnered considerable attention in recent years due to the accelerated advancements in rail transportation engineering. To begin with, urban structures may be adversely affected by ground vibrations that are generated by railroads [1, 2]. Furthermore, the intrusive vibrations and secondary structure noise caused by the high-frequency operation of subways entering and exiting stations negatively affect the quality of life for occupants of over-track areas [3, 4]. Therefore, before installing a new line or retrofitting an existing one, ground vibration assessment is typically mandatory. Complex interactions between tracks, trains, and soil, which may necessitate rigorous analysis, frequently result in exorbitant expenses for these evaluations. Notwithstanding

this, the preservation of vulnerable structures (such as older buildings) could potentially benefit from the ability to forecast vibration levels precisely [5, 6].

With the rapid expansion of urban railroad networks, accurate prediction of railroad-induced vibration levels at ground level and within buildings is required. Current computational methods for predicting railroad-induced ground vibration rely on simplified modeling assumptions that require detailed parameter inputs, which leads to a high degree of uncertainty. Kuo et al. [7] utilized a combination of experimental measurements and numerical simulations for the hybrid prediction of railroad-induced ground vibration.

The effective frequency of transverse rail vibration can reach 1.5 kHz, and longitudinal vibration can reach 2 kHz [8]. A suitable model was developed to study the train–rail

model and to analyze the wheel–rail interaction effects at high frequencies. The proposed 3D moving element method (MEM) track model seems to be suitable for describing the high-frequency dynamics associated with different railroad phenomena.

Recent advances in railroad-induced ground vibration have shown that track–soil interactions play an important role in the low-frequency range. Kouroussis and Verlinden [9] introduced an advanced foundation model at the vehicle/rail subsystem boundary, which allows for high-precision simulation of track/soil interactions. For the analysis of field data registered in the vicinity of vibration sources and buildings at 20 monitoring points (172 samples) in the Lisbon area, Paneiro et al. [10] proposed a multivariate linear regression model for the prediction of ground vibrations caused by underground railroad traffic. Feng et al. [11] used a 3D finite element (FE) model to simulate and analyze the mitigation of ground vibration caused by high-speed trains, investigated the ground vibration caused by the unit load at different speeds and frequencies, and discussed the effects of subgrade treatment and subsoil treatment on vibration isolation. Connolly et al. [12] collated reports that predicted ground vibration levels exceeding national/international permissible limits. The study found that 44% of the reports exceeded the limits in at least one component. This finding shows the importance of railroad vibration assessment for new rail lines, and that ground vibration assessment is an important consideration for most new construction projects.

It is evident that a more accurate method is to study the impacts through field measurements or laboratory tests that replicate the railroad environment. Because of the complexity and nature of the train–track–soil problem, predicting the propagation and intensity of ground effects is not simple. In their study, dos Santos et al. [13] constructed a vehicle–structure–ground system-based numerical model to analyze the trajectory of an Alfa Pendular train traveling at 212 km/hr. Zou et al. [14] conducted field measurements of vibration during metro operation in Shenzhen, China, located in the south of China, where vibration data were collected in five measurement devices considering the train test line and throat area train line as the main sources of vibration in metro stations. The train-induced vibrations were obtained and compared with the limits of the FTA standards. For ground vibration of surface railroad tracks in a combined spatiotemporal and wave number–frequency domain with a very small system matrix, Koroma et al. [15] developed an approximation method for solving linear or nonlinear railroad track–ground interaction problems. An appealing alternative to the utilization of FE and boundary element methods, this approach can be employed to resolve linear or nonlinear railroad track–ground interaction issues with a significantly reduced system matrix. Fully time–space domain discretization is an unattractive alternative.

By employing numerical simulation, the railroad environment can be replicated. A multitude of research groups have devised diverse modeling techniques for numerical simulation utilizing boundary element and finite element methods. Their objective is to comprehend the propagation of

railway-induced vibrations by analyzing the mechanisms that generate such vibrations. Shi et al. [16] conducted a theoretical investigation on the impact of the dynamic response of railroad viaducts. They utilized the periodic structure of the track, specifically the parametric excitation caused by the periodic passage of moving wheels through the foundation. To solve the interaction problem between a moving wheel and an infinite track, they employed the Fourier series method, which involves representing the wheel–rail forces and displacements at the contact points as periodic functions of time [17]. Rigueiro et al. [18] conducted a numerical study of the dynamic response of a midspan railroad viaduct using the response acceleration measurements of the viaduct. Lopes et al. [19] carried out the effect of soil stiffness on vibrations of buildings induced by railroad traffic in tunnels, simulating vibration sources (train–track interaction), vibration propagation (tunnel–surface system), and vibration reception (buildings close to the railroad infrastructure) by means of a substructural approach. It was found that soil stiffness plays an important role in the vibration propagation mechanism in the ground and the interaction between soil and structures. Lai et al. [20] proposed that creating a thorough prediction tool for ground vibration caused by railroads should take into account three main aspects: the source problem concerning train–track dynamics, the propagation problem involving the transfer of vibrations from source to receiver, and the structural response problem related to soil–structure dynamics caused by vibrations from nearby railroad facilities arising from the dynamic interplay between soil and structure.

As a significant indicator for determining the operational condition of bridges, the dynamic response of bridges to passing railroads is regarded as critical. When considering the overall behavior of a bridge, including factors such as load-carrying capacity, structural rigidity, and the extent of damage, bridge displacements are among the most valuable indicators of structural health. In order to accurately distinguish bridge damage, Baba and Kondoh [21] conducted vibration experiments on fixed beams positioned at both ends of a simulated bridge and proposed a method for monitoring bridge health utilizing impedance-loaded surface acoustic wave sensors, which was accomplished through the application of unsupervised machine learning. Saidin et al. [22] used ambient vibration testing to obtain vibration response measurements to determine the dynamic properties of the structure. The study compares three modal detection methods: frequency domain decomposition, enhanced frequency domain decomposition, and stochastic subspace identification. Identification and the modal shapes of each method are verified using modal assurance criterion values to validate the accuracy of the results. Jayasundara et al. [23] damage indices obtained from vibration data were used as input data for neural network training and validation for damage detection, localization, and quantification of structural bridge components.

Using the maximum wheel load reduction rate of the train on the bridge as an illustration, Zhang et al. [24] collected a sample set of the train–bridge system’s maximum dynamic response and analyzed its statistical characteristics. Koroma et al. [15] used space–time and wave number frequency domain modeling

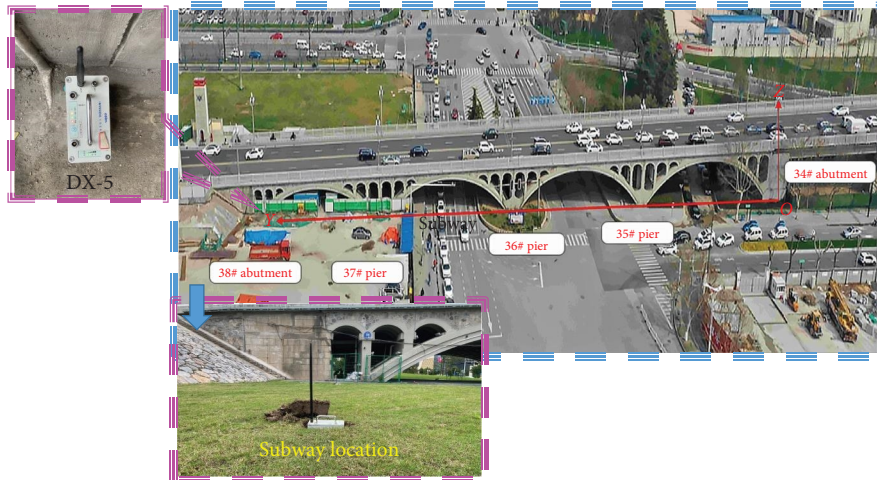


FIGURE 1: Relationship between subway and plan position of hyperbolic arch bridge.

techniques to predict ground vibration of above-ground railroad tracks. The FE method was used to model the railroad track in the space–time domain and the ground in the wave number frequency domain. The results of time-range and spectral analyses of track vibration, interaction force, and free-field ground vibration for the coupled track/ground model are given. Xu et al. [25] developed a 3D hybrid model for simulating the dynamic track–tunnel–soil interaction in a ballasted underground. Kuo et al. [7] used field measurements to predict railroad-induced ground and building vibration levels.

In order to characterize the ground vibration in the time domain, Feng et al. [11] constructed a 3D model utilizing the FE method. Material damping is modeled using the absorbing boundary technique, while wave reflection from artificial edges is prevented using the Rayleigh damping method. An examination of unit load-induced ground vibration at various velocities and frequencies is presented. dos Santos et al. [13] presented an experimental validation of a numerical model for predicting vibrations in railroad traffic. The model takes into account the dynamic interaction of the vehicle–structure–ground system and can be used for a full 3D analysis of vibration problems caused by railroad traffic. Onat [26] collected data from the literature on historical masonry bridges and proposed an empirical formula for the sensitive assessment of modal characteristics such as intrinsic frequency. Bayraktar et al. [27] studied eight historic masonry arch bridges of different spans and gave the test frequencies, modal shapes, and damping ratios of the historic masonry arch bridges.

The issue of ground vibration induced by subway train operations is increasingly becoming a significant concern. In order to address the unpredictability of the train–track–tunnel–soil–structures system, a vibration assessment via long-term monitoring is necessary. This evaluation aims to examine the effects of vibration on inhabitants, sensitive equipment, and buildings and to provide a foundation for designing measures to reduce vibration. The focus of this work is the approach bridge of the Nanjing Yangtze River Bridge, which

is designed as a double-curved arch bridge. This kind of bridge construction is unique and has a high susceptibility to deformation produced by external forces. The Nanjing Yangtze River Bridge has been safely operational for over 50 years. Over time, the bridge foundation and structure have undergone varying degrees of deformation accumulation. Therefore, a more rigorous assessment of the impacts of nearby subway operations on the bridge is necessary.

This paper’s innovative content is as follows: This paper utilizes the new Nanjing Metro Line 8, which crosses the Nanjing Yangtze River Bridge highway bridge, to conduct dynamic tests on rail transportation vibration on the old bridge. The purpose is to identify, pinpoint, and measure potential damage to the structural components of the arch bridge in the future. A 3D numerical simulation model of “bridge–soil–tunnel” was created to analyze the combined effects of foundation pit excavation and shield tunnel crossing construction on the Nanjing Yangtze River Bridge. The goal is to ensure the safety of deep foundation pit and shield tunneling construction in a complex and sensitive environment and minimize the impacts on sensitive structures nearby, such as the Yangtze River Bridge and the double-curved arch bridge. The goal is to guarantee the safety of deep foundation and shield tunneling construction in a complex and sensitive environment, reduce the impact on the nearby sensitive structure—the Yangtze River Bridge, and offer guidance for similar projects in the Yangtze River floodplain.

2. Over-Track Building and Metro Description

2.1. Double-Curved Arch Bridge Overview. Nanjing Yangtze River Bridge’s north approach hyperbolic arch bridge was completed in 1968, with a total of four holes ($3 \times 34.9 + 32.3$) and a total length of 137 m. Each hole is an equal cross-section suspension chain line hingeless arch, with a vector span ratio of $1/4$ – $1/5$. Figure 1 shows the subway and the hyperbolic arch bridge plan position relationship diagram.

The main arch ring of the hyperbolic arch bridge superstructure consists of 16 arch ribs and 15 arch waves. The arch

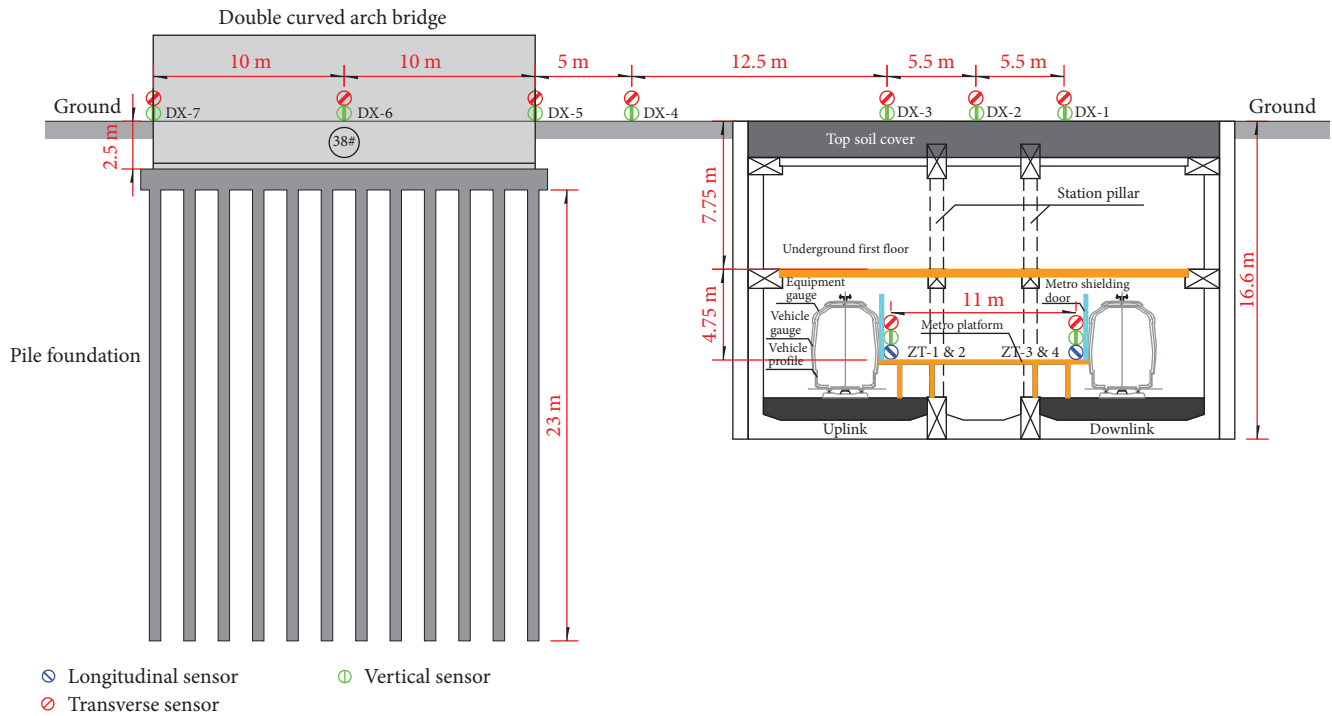


FIGURE 2: Relationship between subway and hyperbolic arch bridge elevation position.

rib is 250 grade reinforced concrete precast structure, the center spacing 1.3 m, the total width of the group rib is 19.76 m; the arch wave is 200 precast concrete structure, the system of arc arch, the arch wave is 6 cm thick, the net span diameter is 1.04 m, the ratio of the vector span is 1/3; the arch plate is filled with 300 cast-in-place components, and the arch wave to form an integral whole; the transverse connecting rods between the arch ribs are precast components, the section is 8 cm × 11 cm, the maximum spacing is 1.8 m, the reinforcement is added 25 cm × 38 cm section. The maximum spacing of connecting rods is 1.8 m, and large tie rods with cross-sections of 25 cm × 38 cm (1–3 rods per hole) are added for reinforcement. The foundation form of the hyperbolic arch bridge is a group pile foundation, with a pile length of 23 m and a pile diameter of 0.6 m.

2.2. Metro Depot Description. The foundation pit of Nanjing Metro Line S8 South Extension Project Yangtze River Bridge North Station is adjacent to the hyperbolic arch bridge and located on the west side of the hyperbolic arch bridge. It is side by side with Pier 37# and Pier 38# of the hyperbolic arch bridge. Figure 2 shows the subway and hyperbolic arch bridge elevation location relationship. The subway line was completed and successfully opened to traffic at the end of September 2022, and the train adopts a B-type drum train with four sections; each section is 19 m long, 2.88 m wide, and 3.8 m high, with a maximum operating speed of 120 km/hr.

3. Measurement Program

The following specifications inform the test program and vibration monitoring standards presented in this paper: (i) GB 10070-88 Standard of environmental vibration in urban

areas [28], (ii) GB 3096-2008 Environmental quality standard for noise [29], and (iii) JGJ/T 170-909 Standard for limit and measuring method of building vibration and secondary noise caused by urban rail transit [30].

The field test was conducted from September 19 to 22, 2023, in the vicinity of the North Station of the Yangtze River Bridge on the Nanjing Metro Line S8 South Extension Project. Testing was conducted on the vibration induced by running trains and the bridge's vertical, transverse, and longitudinal movement due to subway operation, resulting in a significant quantity of test data.

3.1. Measurement Point Arrangement. The tests in this study include the self-oscillation frequency of the bridge, the site response under the influence of the operation of Metro Line S8, and the response of the sensitive parts of the hyperbolic arch bridge. Response measurements include transverse/vertical acceleration and displacement. Specifically include:

- (1) This paper focuses on the construction of over-track buildings with a unique spatial relationship. In order to measure the effects of this construction, four measurement points were strategically placed along the vertical and horizontal lines of the subway station. The specific locations of these points can be seen in Figures 1 and 2. Horizontally, the points ZT-01 and ZT-03 were arranged, while vertically, the points ZT-02 and ZT-04 were arranged.
- (2) A transverse vibration response test is conducted in the vicinity of pier 38# of the hyperbolic arch bridge, with measurement points placed as depicted in Figure 3. There are a total of eight measurement

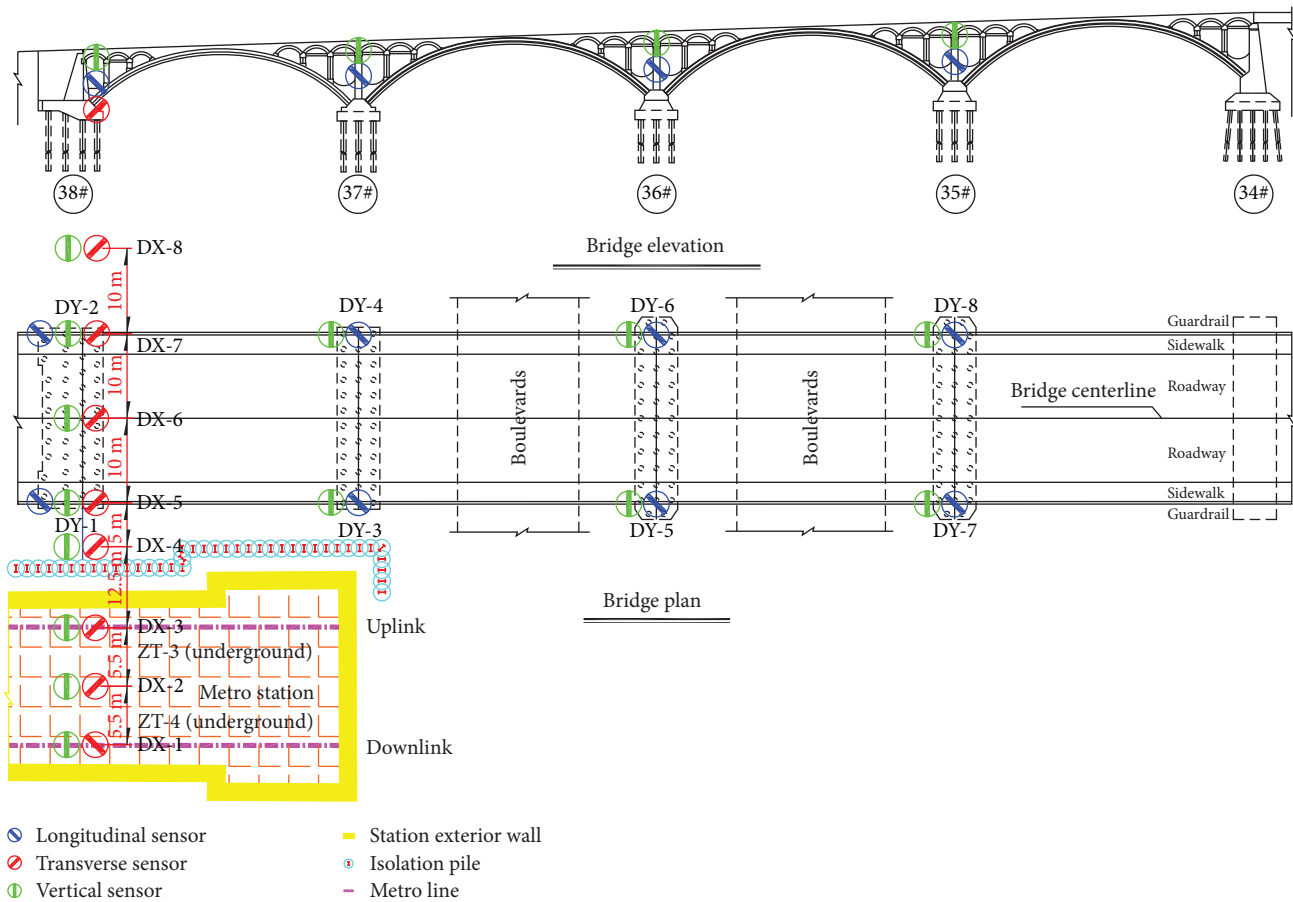


FIGURE 3: Layout of measurement points.

points positioned from the surface above the subway line toward the bridge. Among these, DX-5, DX-6, and DX-7 are situated on the abutment.

- (3) The study involves conducting a longitudinal vibration response test at the arch foot of 35–38# holes of a hyperbolic arch bridge. The measurement points, as illustrated in Figure 3, consist of a total of eight points. Additionally, the 34# piers are elevated from the ground, and the measurement points are not arranged in a specific manner. This work specifically examines the transverse vibration response of the bridge. It is important to mention that the scope of this paper does not include a detailed discussion of longitudinal vibration research in relation to the bridge.

3.2. Testing Instruments. The field testing of bridge vibrations induced by subway train operation was the subject of this investigation; the instruments utilized for the assessments are detailed in Table 1. The field measurements were conducted utilizing 12 accelerometer instruments. As depicted in Figures 4–7, the acceleration and velocity time-history, as well as Fourier amplitude spectra, were acquired for the location within 48.5 m of the subway track line and over-track building in this investigation.

4. Vibration Response on the Metro and Over-Track Building

4.1. Subway Vibration Response. Figure 4 displays the Fourier spectrum and decibel diagrams of the ground vibration acceleration time-history curves caused by a subway train and its reaction to a passing passenger automobile traveling at 80 km/hr. The experiments in this research were done during regular subway operation, not during preoperation load testing. Hence, the operating speed referred to is the typical pace at which subways operate.

Figure 4 illustrates that the subway vibration frequency ranges from 51 to 55 Hz. Studies have shown that frequencies of 50–63 Hz related to the foundation, interior vibration, and secondary noise are the dominant ones [31]. Specifically, indoor structures, such as station buildings, are intensified at 40–63 Hz. Hence, it is necessary to decrease the indoor secondary noise by reducing the wheel and rail vibration frequency from 50 to 63 Hz [32].

As per the guidelines provided by GB 3096 Environmental quality standard for noise [29], DB11/T 838-2019 Code for application technique of metro noise and vibration control [33], and sound insulation design code for civil buildings standard of environmental vibration in urban area [34], the metro vibration should produce noise levels no higher than 70 dB. The test demonstrates that the environmental vibration

TABLE 1: Dynamic load test equipments.

Serial no.	Equipment name	Product specification	Quantity
1	Wireless vibration collector	INV9580	12
2	Horizontal vibration sensor	941B	6
3	Vertical vibration sensor	941B	6
4	Dynamic signal test system	DH3817J	2

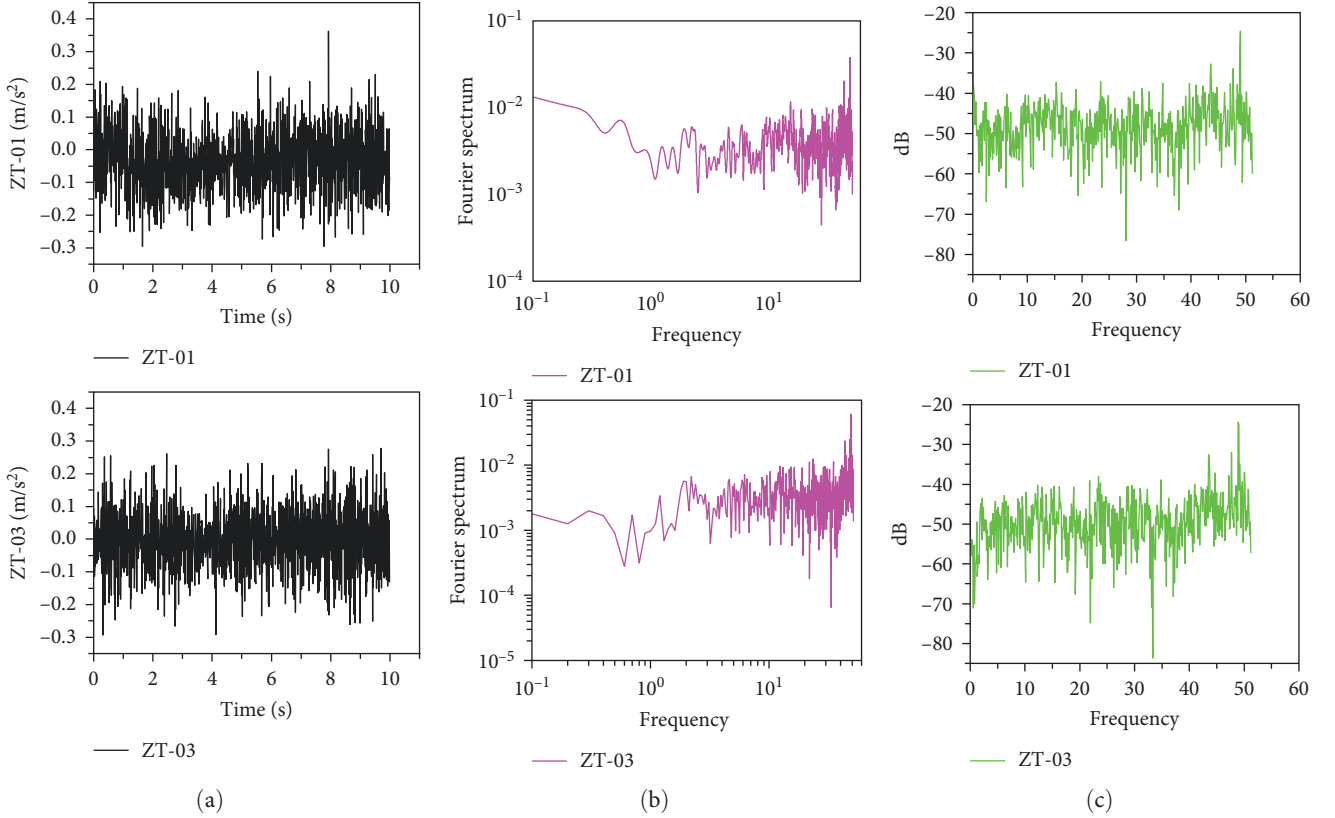


FIGURE 4: Time-history curves of ground vibration acceleration and corresponding Fourier spectra of subway train when 80 km/hr passenger car passes. (a) Time-history curves, (b) corresponding Fourier spectra, and (c) dB charts.

brought on by the subway vibration satisfies the code's standards.

4.2. Bridge Vibration Response. The transverse vibration acceleration time-history curves of the bridge vibration and its response during the passage of a 100 km/hr passenger car are illustrated in Figure 5 through Fourier spectra and dB diagrams. It is important to mention that the experiments performed in this research were carried out during regular subway operations and not preoperational stress evaluations. The operational pace is thus the speed at which the subway normally operates.

As to the code for rating existing railway bridges (railway transportation letter (2004) No. 120) [35], the transverse vibration acceleration of the bridge span structure in the plane of loading shall not surpass 1.4 m/s^2 while a train is passing through. Figure 5 illustrates that the acceleration of the lateral vibration of the bridge exceeds 1.4 m/s^2 . The Nanjing Yangtze River Bridge and its northern approach

bridge, with a hyperbolic arch construction, began operating in September 1968. It continues to serve as a vital traffic link between Nanjing's main city and the Jiangbei New Area. The test findings indicate that the hyperbolic arch construction, which has been in service for almost 54 years, has internal damage. The bridge is a significant cultural heritage site in Nanjing and cannot be removed; it can only be restored and strengthened.

5. Vibration Reduction Measures

As urban construction progresses, an increasing number of deep foundation structures, such as bridges, are being built near clusters of tunnels. The excavation of the pit, construction of the shield tunnel crossing, and operation of the subway will have an impact on the nearby pile foundation. Specifically, it will affect the safety and deformation of the bridge bearing on the pile foundation. To mitigate this impact, the project incorporates additional protective measures to

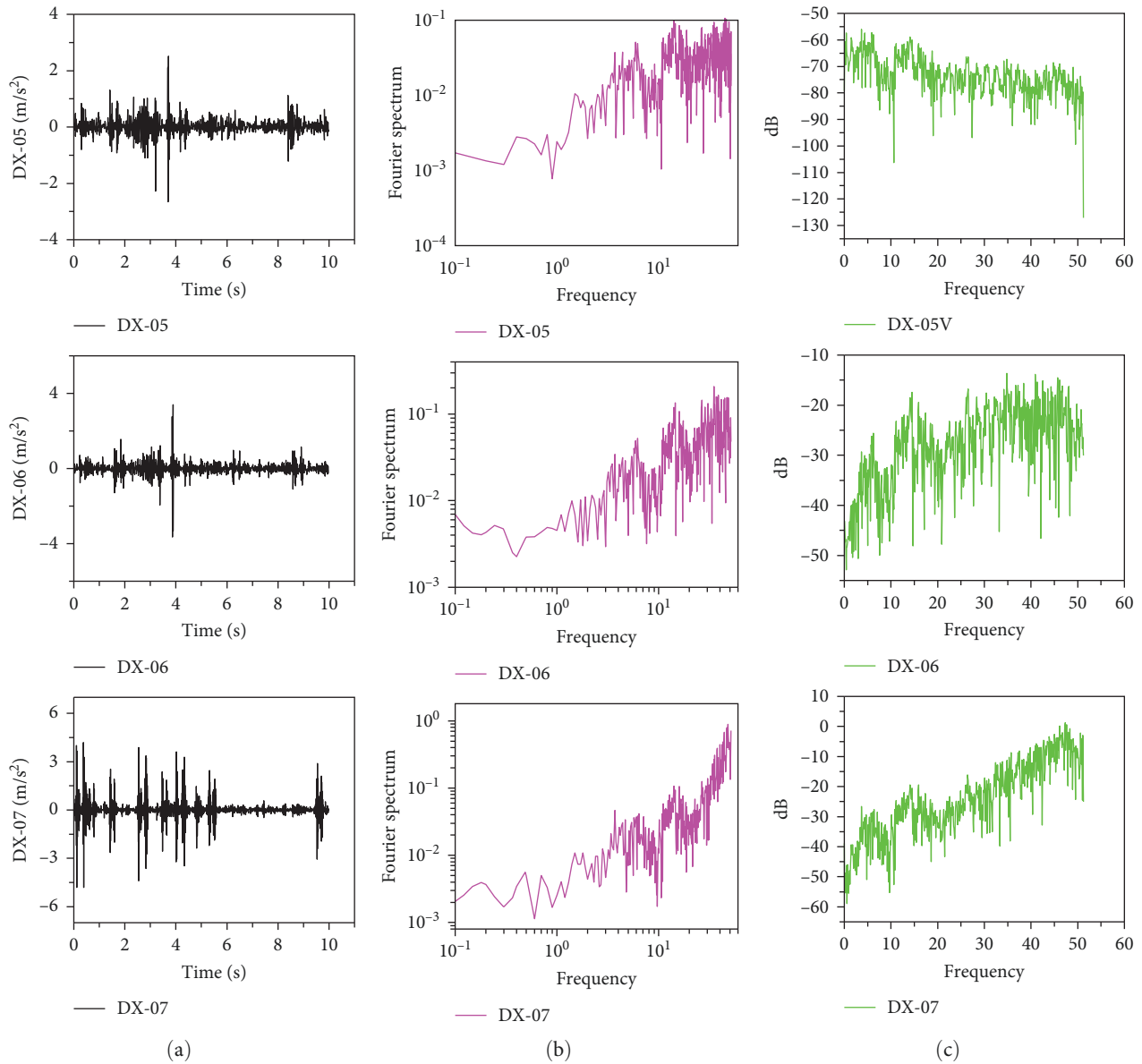


FIGURE 5: Time-history curves and corresponding Fourier spectra of lateral acceleration of bridge without vibration reduction measure when 80 km/hr passenger car passes. (a) Time-history curves, (b) corresponding Fourier spectra, and (c) dB charts.

enhance the stiffness of the soil [36, 37]. This paper explores the use of vibration control measures, specifically isolation pile protection and metro jet system (MJS) reinforcement, in subway construction. The MJS system is an improved method based on the original spray-mixing technique. By using this method, the disturbance to the soil layer surrounding the reinforced soil can be minimized during construction [38]. Research has shown that the timely use of MJS isolation piles, which are installed with low disturbance, may successfully reduce the impact of excavation on structural deformation when constructing deep foundations near groups of tunnels [39]. This part aims to further study the impact of MJS isolation piles on reducing the vibration of the nearby structure by analyzing the deformation response of these piles to both the structure and the ground in the tunnel.

The previous test conducted in 4.2 indicated that the lateral vibration acceleration of the bridge was above the stipulated threshold. In order to minimize the effects of the Metro Line 8 construction on the double curving arch bridge of the Yangtze River Bridge, appropriate measures must be implemented to reduce vibrations. Indeed, while constructing the subway, the potential disruption caused by the excavation of deep and large pits on the Nanjing Yangtze River Bridge was anticipated. In order to mitigate this, MJS isolation piles were installed between the pits and the bridge piles to minimize any deformation of the bridge piles resulting from the pit excavation. Based on the comparative study of the positioning of isolation piles, it is recommended that the isolation piles be placed as near as feasible to the foundation pit. MJS isolation piles are used to strengthen the vertical

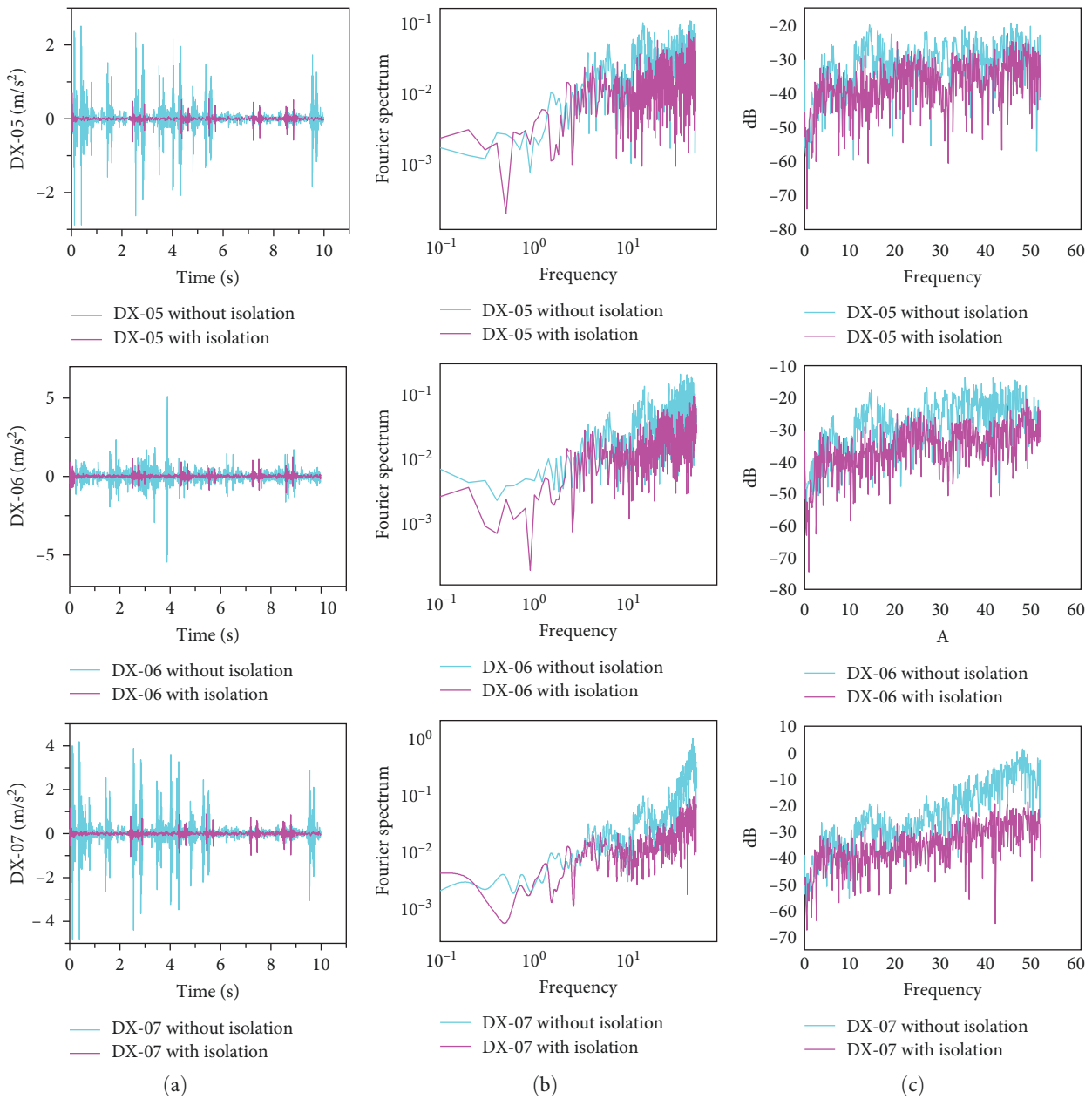


FIGURE 6: Time-history curves and corresponding Fourier spectra of lateral acceleration of bridge with vibration reduction measure when 80 km/hr passenger car passes. (a) Time-history curves, (b) corresponding Fourier spectra, and (c) dB charts.

section of the subway tunnel, namely the portion located between the tunnel and the double-curved arch bridge. These piles are spaced at intervals of $\Phi 1200@900$. Figure 8 displays the measurements of the MJS isolation piles and their arrangement in relation to the subway and the double-curved arch bridge. The section of the MJS isolation piles that falls beyond the focus of this study will not be extensively discussed. However, we will provide a brief explanation of the project's origins. This research only examines the impact of MJS isolation piles on the regulation of vibration in the nearby structure.

Dynamic measurements were conducted on the bridge using isolation piles. Figure 6 displays the time-range curves of transverse vibration acceleration of the bridge before and

after implementing isolation measures. Additionally, it shows the Fourier spectra and dB plots of the bridge's responses when a passenger car traveling at a speed of 100 km/hr passes through. The test results indicate that the use of MJS isolation piles for reinforcement has led to a reduction in the transverse vibration of the bridge. Specifically, the acceleration at the DX-5 measurement point is 1.35 m/s^2 , the acceleration at the DX-6 measurement point is 1.25 m/s^2 , and the acceleration at the DX-7 measurement point is 1.16 m/s^2 . These values meet the specification requirements.

Based on the field test, the bridge's first-order self-vibration frequency is of the antisymmetric vibration type and has a frequency of 8.79 Hz. Figure 7 depicts the temporal progression

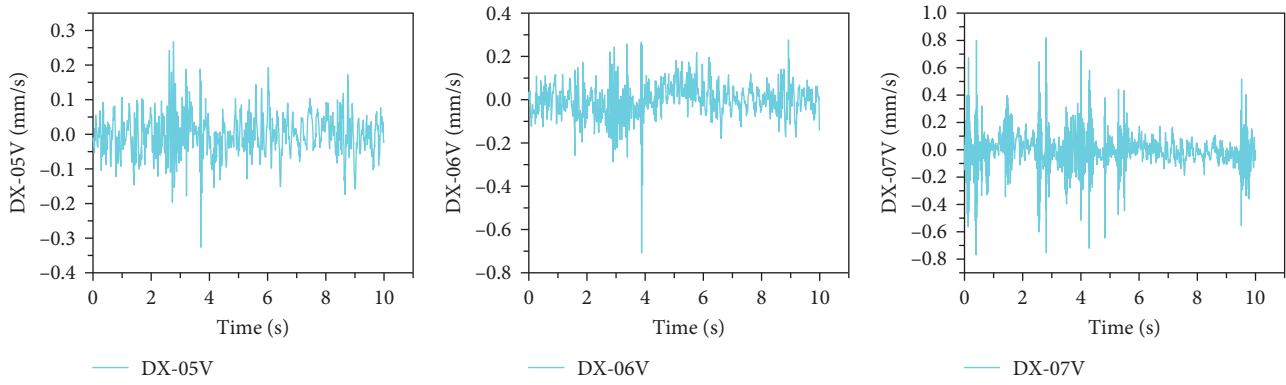
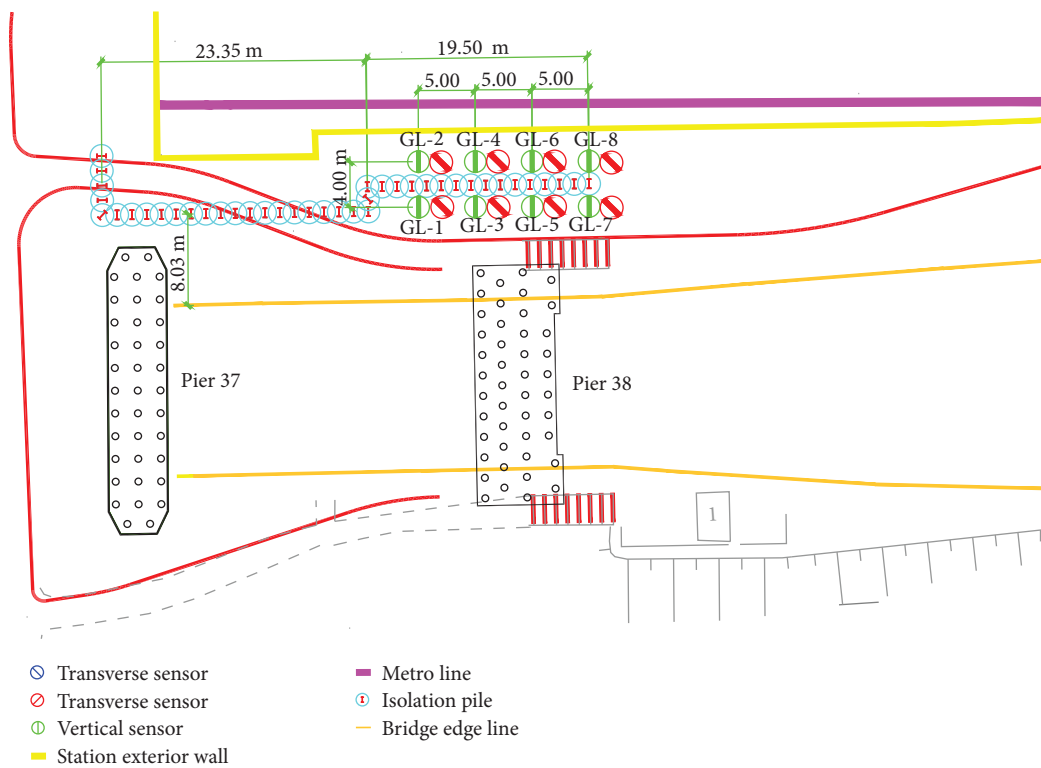
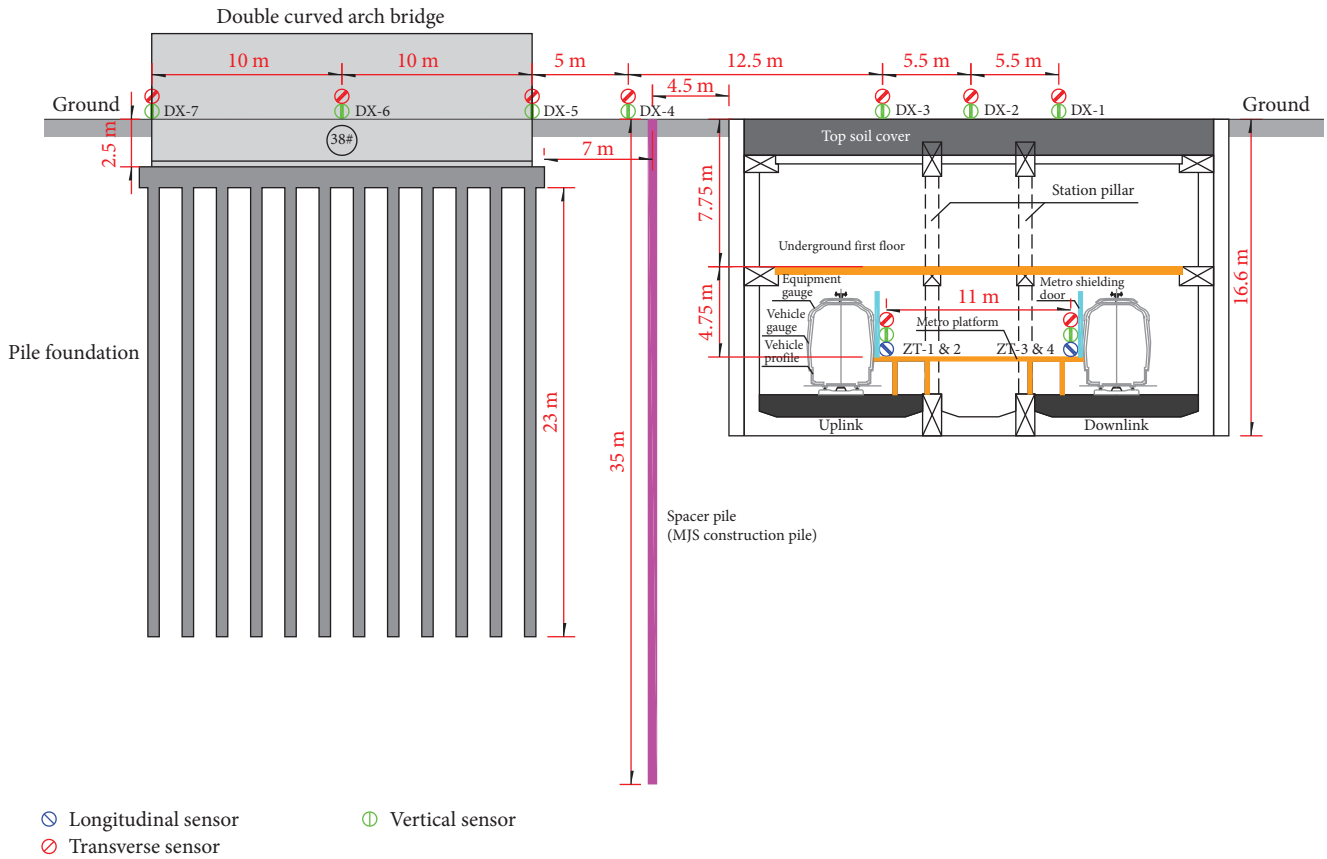


FIGURE 7: Time-history curves of transverse velocity of bridge vibration after adapting vibration reduction measures when 80 km/hr passenger car passes through.



(a)

FIGURE 8: Continued.



(b)

FIGURE 8: MJS isolation pile vibration reduction: (a) layout plan; (b) tunnel and bridge pile position profile schematic.

TABLE 2: Vibration impact assessment of vibration-sensitive buildings.

Building type	Peak permissible vibration velocity at the top (mm/s)	
	1–100 Hz	1–10 Hz
Frequency (Hz)		
Industrial buildings, public buildings	10	5
Residential buildings	5	2
Buildings that are sensitive to vibration have conservation value and cannot be classified into the above two categories	2.5	1.0

of the lateral velocity of the bridge oscillation after the implementation of isolation measures in response to the passage of a passenger automobile traveling at a speed of 100 km/hr. Based on the GB 10070-88 standards for urban environmental vibration [28], the assessment of vibration impact on vibration-sensitive buildings and other impacts is presented in Table 2. The table indicates that the transverse vibration of the bridge is greatly reduced when MJS isolation piles are used, satisfying the specification requirements.

6. Conclusions

In this study, a field test was carried out on Nanjing Metro 8, within 48.5 m from the line, to test the bridge vibration caused by running subway trains. A large amount of experimental data was obtained. Some meaningful conclusions were drawn

through the analysis of the data in the frequency domain, providing experimental data for the study of the propagation of the environmental vibration law:

- (1) The vibration level of vertical ground acceleration caused by running train speed in the range of 80–120 km/hr is generally 60–110 dB; the horizontal vibration level of vertical line is 50–95 dB; and the horizontal vibration level of parallel line is 55–80 dB. The horizontal vibration level of parallel lines is 55–80 dB.
- (2) Prior to the building of the subway, testing revealed that the bridge without MJS isolation piles (referring to the bridge in its original state) had internal structural damage. This damage caused the bridge to undergo transverse vibration acceleration exceeding

1.4 m/s². Hence, it is essential to implement vibration control measures for the bridge.

- (3) The bridge's dynamics were analyzed using MJS isolation piles, and the tests demonstrated a significant reduction in transverse vibration, therefore satisfying the stated standards.
- (4) The findings of this research suggest that MJS isolation piles may be regarded as a viable choice for implementing measures to limit vibrations.

Data Availability

The data used to support the findings of this study are available from the corresponding author upon request.

Conflicts of Interest

The authors declare that have no conflicts of interest.

Authors' Contributions

Yuan Xu, Hui Li, and Lingkun Chen contributed to conceptualization, visualization, and project administration. Yuan Xu and Lingkun Chen contributed to methodology and writing—original draft preparation. Yuan Xu, Hui Li, Jue Hou, Liming Zhu, and Lingkun Chen contributed to software. Yuan Xu, Liming Zhu, and Lingkun Chen contributed to validation. Jue Hou, Liming Zhu, and Lingkun Chen contributed to formal analysis. Lingkun Chen contributed to resources, supervision, and funding acquisition. Lingkun Chen and Yuan Xu contributed to data curation. Yuan Xu, Hui Li, Jue Hou, Liming Zhu, and Lingkun Chen contributed to writing—review and editing. All authors have read and agreed to the published version of the manuscript. Yuan Xu and Lingkun Chen contributed equally to this work.

Acknowledgments

The corresponding author thanks the 2018 Jiangsu Provincial Government Scholarship Program (no. 228) for supporting his visit to the University of California, Los Angeles. This paper is part of the research work of the National Key R&D Project of China (grant nos. 2021YFB2600602 and 2021YFB2600600). The corresponding author would like to gratefully acknowledge the support for this research by the Yangzhou Key R&D Program (Social Development) grant no YZ2023077.

References

- [1] C. Zou, J. A. Moore, M. Sanayei, Z. Tao, and Y. Wang, "Impedance model of train-induced vibration transmission across a transfer structure into an over-track building in a metro depot," *Journal of Structural Engineering*, vol. 148, no. 11, Article ID 04022187, 2022.
- [2] Y. Qiu, C. Zou, J. Hu, and J. Chen, "Prediction and mitigation of building vibrations caused by train operations on concrete floors," *Applied Acoustics*, vol. 219, Article ID 109941, 2024.
- [3] X. Huang, Z. Zeng, D. Wang, X. Luo, P. Li, and W. Wang, "Experimental study on the vibration reduction characteristics of the floating slab track for 160 km/h urban rail transit," *Structures*, vol. 51, pp. 1230–1244, 2023.
- [4] Z. Tao, Y. Wang, M. Sanayei, J. A. Moore, and C. Zou, "Experimental study of train-induced vibration in over-track buildings in a metro depot," *Engineering Structures*, vol. 198, Article ID 109473, 2019.
- [5] G. Kouroussis, K. E. Vogiatzis, and D. P. Connolly, "A combined numerical/experimental prediction method for urban railway vibration," *Soil Dynamics and Earthquake Engineering*, vol. 97, pp. 377–386, 2017.
- [6] D. P. Connolly, G. Kouroussis, O. Laghrouche, C. L. Ho, and M. C. Forde, "Benchmarking railway vibrations—track, vehicle, ground and building effects," *Construction and Building Materials*, vol. 92, pp. 64–81, 2015.
- [7] K. A. Kuo, H. Verbraken, G. Degrande, and G. Lombaert, "Hybrid predictions of railway induced ground vibration using a combination of experimental measurements and numerical modelling," *Journal of Sound and Vibration*, vol. 373, pp. 263–284, 2016.
- [8] J. Martínez-Casas, J. Giner-Navarro, L. Baeza, and F. D. Denia, "Improved railway wheel-track interaction model in the high-frequency domain," *Journal of Computational and Applied Mathematics*, vol. 309, pp. 642–653, 2017.
- [9] G. Kouroussis and O. Verlinden, "Prediction of railway ground vibrations: accuracy of a coupled lumped mass model for representing the track/soil interaction," *Soil Dynamics and Earthquake Engineering*, vol. 69, pp. 220–226, 2015.
- [10] G. Paneiro, F. O. Durão, M. C. Silva, and P. F. Neves, "Prediction of ground vibration amplitudes due to urban railway traffic using quantitative and qualitative field data," *Transportation Research Part D: Transport and Environment*, vol. 40, pp. 1–13, 2015.
- [11] S.-J. Feng, X.-L. Zhang, Q.-T. Zheng, and L. Wang, "Simulation and mitigation analysis of ground vibrations induced by high-speed train with three dimensional FEM," *Soil Dynamics and Earthquake Engineering*, vol. 94, pp. 204–214, 2017.
- [12] D. P. Connolly, G. P. Marecki, G. Kouroussis, I. Thalassinakis, and P. K. Woodward, "The growth of railway ground vibration problems—a review," *Science of the Total Environment*, vol. 568, pp. 1276–1282, 2016.
- [13] N. C. dos Santos, J. Barbosa, R. Calçada, and R. Delgado, "Track-ground vibrations induced by railway traffic: experimental validation of a 3D numerical model," *Soil Dynamics and Earthquake Engineering*, vol. 97, pp. 324–344, 2017.
- [14] C. Zou, Y. Wang, J. A. Moore, and M. Sanayei, "Train-induced field vibration measurements of ground and over-track buildings," *Science of the Total Environment*, vol. 575, pp. 1339–1351, 2017.
- [15] S. G. Koroma, D. J. Thompson, M. F. M. Hussein, and E. Ntotsios, "A mixed space-time and wavenumber-frequency domain procedure for modelling ground vibration from surface railway tracks," *Journal of Sound and Vibration*, vol. 400, pp. 508–532, 2017.
- [16] L. Shi, Y. Cai, P. Wang, and H. Sun, "A theoretical investigation on influences of slab tracks on vertical dynamic responses of railway viaducts," *Journal of Sound and Vibration*, vol. 374, pp. 138–154, 2016.
- [17] X. Sheng, C. J. C. Jones, and D. J. Thompson, "Responses of infinite periodic structures to moving or stationary harmonic loads," *Journal of Sound and Vibration*, vol. 282, no. 1-2, pp. 125–149, 2005.
- [18] C. Rigueiro, C. Rebelo, and L. S. da Silva, "Influence of ballast models in the dynamic response of railway viaducts," *Journal of Sound and Vibration*, vol. 329, no. 15, pp. 3030–3040, 2010.

- [19] P. Lopes, P. A. Costa, R. Calçada, and A. S. Cardoso, "Influence of soil stiffness on building vibrations due to railway traffic in tunnels: numerical study," *Computers and Geotechnics*, vol. 61, pp. 277–291, 2014.
- [20] C. Lai, A. Callerio, E. Faccioli, V. Morelli, and P. Romani, "Prediction of railway-induced ground vibrations in tunnels," *Journal of Vibration and Acoustics*, vol. 127, no. 5, pp. 503–514, 2005.
- [21] S. Baba and J. Kondoh, "Damage evaluation of fixed beams at both ends for bridge health monitoring using a combination of a vibration sensor and a surface acoustic wave device," *Engineering Structures*, vol. 262, Article ID 114323, 2022.
- [22] S. S. Saidin, S. A. Kudus, A. Jamadin et al., "Operational modal analysis and FE model updating of ultra-high-performance concrete bridge based on ambient vibration test," *Case Studies in Construction Materials*, vol. 16, Article ID e01117, 2022.
- [23] N. Jayasundara, D. P. Thambiratnam, T. H. T. Chan, and A. Nguyen, "Damage detection and quantification in deck type arch bridges using vibration based methods and artificial neural networks," *Engineering Failure Analysis*, vol. 109, Article ID 104265, 2020.
- [24] X. Zhang, Y. Han, L. Wang, H. Liu, and C. S. Cai, "An adaptive surrogate model approach for random vibration analysis of the train–bridge system," *Engineering Structures*, vol. 278, Article ID 115490, 2023.
- [25] Q.-Y. Xu, X. Ou, F. T. K. Au, P. Lou, and Z.-C. Xiao, "Effects of track irregularities on environmental vibration caused by underground railway," *European Journal of Mechanics—A/Solids*, vol. 59, pp. 280–293, 2016.
- [26] O. Onat, "Impact of mechanical properties of historical masonry bridges on fundamental vibration frequency," *Structures*, vol. 27, pp. 1011–1028, 2020.
- [27] A. Bayraktar, T. Türker, and A. C. Altunişik, "Experimental frequencies and damping ratios for historical masonry arch bridges," *Construction and Building Materials*, vol. 75, pp. 234–241, 2015.
- [28] State Environmental Protection Administration, *Standard of Environmental Vibration in Urban Area GB 10070-88*, China Standard Press, Beijing, 1988.
- [29] Ministry of Ecology and Environment and People's Republic of China, *Environmental Quality Standard for Noise GB3096-2008*, China Environmental Science Press, Beijing, 2008.
- [30] Ministry of Housing and Urban-Rural Development and People's Republic of China, *JGJ/T 170-2009 Standard for Limit and Measuring Method of Building Vibration and Secondary Noise Caused by Urban Rail Transit*, China Construction Industry Press, Beijing, 2008.
- [31] Y.-Y. Ko, L.-Y. Lai, G.-H. Lee, Y.-F. Wang, S.-W. Jao, and T.-F. Fu, "Experimental study on construction vibration during different phases of diaphragm wall-supported deep excavation and its influence on indoor sensitive receivers," *Journal of Vibration and Control*, vol. 29, no. 17-18, pp. 3925–3941, 2023.
- [32] J. Zheng, X. Li, X. Zhang, R. Bi, and X. Qiu, "Structure-borne noise of fully enclosed sound barriers composed of engineered cementitious composites on high-speed railway bridges," *Applied Acoustics*, vol. 192, Article ID 108705, 2022.
- [33] DB11/T838-2019, *Beijing Rail Transit Design and Research Institute Co. Code for Application Technique of Metro Noise and Vibration Control*, Beijing Municipal Administration of Market Supervision, Beijing, 2019.
- [34] Ministry of Housing and Urban-Rural Development of the People's Republic of China, *GB50118-2010, Sound Insulation Design Code for Civil Buildings Standard of Environmental Vibration in Urban Area*, China Building Industry Press, Beijing, 2010.
- [35] W. Liu, Z. Wu, C. Li, and L. Xu, "Prediction of ground-borne vibration induced by a moving underground train based on excitation experiments," *Journal of Sound and Vibration*, vol. 523, Article ID 116728, 2022.
- [36] H. Li, C. He, Q. Gong, S. Zhou, X. Li, and C. Zou, "TLM-CFSPML for 3D dynamic responses of a layered transversely isotropic half-space," *Computers and Geotechnics*, vol. 168, Article ID 106131, 2024.
- [37] C. He, S. Zhou, and P. Guo, "Mitigation of railway-induced vibrations by using periodic wave impeding barriers," *Applied Mathematical Modelling*, vol. 105, pp. 496–513, 2022.
- [38] Z. Xiao, S. Xie, A. Hu, Y. Chen, and M. Wang, "Displacement control in irregular deep excavation adjacent to tunnel groups in structural soil: a case study of MJS cement-soil composite piles and grouting rectification," *Case Studies in Construction Materials*, vol. 20, Article ID e03085, 2024.
- [39] Q. Yang, B. Wang, and W. Guo, "Effects of large-diameter shield tunneling on the pile foundations of high-speed railway bridge and soil reinforcement schemes," *Symmetry*, vol. 14, no. 9, Article ID 1913, 2022.